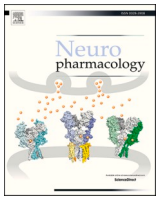
Neuropharmacology 198 (2021) 108755



Contents lists available at ScienceDirect

Neuropharmacology

journal homepage: www.elsevier.com/locate/neuropharm





Neuron-specific responses to acetylcholine within the spinal dorsal horn circuits of rodent and primate

Matthew J. Sykes [a,b], Orsolya S. Kekesi [a,b], Yan T. Wong [a,b,c], Fei-Yue Zhao [d], David Spanswick [a,b,e], Wendy L. Imlach [a,b,*]

[a] Department of Physiology, Monash University, Melbourne, VIC, 3800, Australia
[b] Monash Biomedicine Discovery Institute, Melbourne, VIC, 3800, Australia
[c] Department of Electrical and Computer Systems Engineering, Melbourne, VIC, 3800, Australia
[d] NeuroSolutions Ltd, Coventry, CV4 7AL, United Kingdom
[e] University of Warwick, Warwick Medical School, Coventry, CV4 7AL, United Kingdom

ARTICLE INFO

Keywords:
Acetylcholine
Pain
Dorsal horn
Spinal cord
Synaptic transmission
Cholinergic modulation

ABSTRACT

Excitatory and inhibitory neurotransmission within the spinal dorsal horn is tightly controlled to regulate transmission of nociceptive signals to the brain. One aspect of this control is modulation of neuronal activity through cholinergic signaling. Nociceptive neurons in the dorsal horn express both nicotinic and muscarinic cholinergic receptors and activation of these receptors reduces pain in humans, while inhibition leads to nociceptive hypersensitivity. At a cellular level, acetylcholine (ACh) has diverse effects on excitability which is dependent on the receptor and neuronal subtypes involved. In the present study we sought to characterize the electrophysiological responses of specific subsets of lamina II interneurons from rat and marmoset spinal cord. Neurons were grouped by morphology and by action potential firing properties. Whole-cell voltage-clamp recordings from lamina II dorsal horn neurons of adult rats showed that bath applied acetylcholine increased, decreased or had no effect on spontaneous synaptic current activity in a cell-type specific manner. ACh modulated inhibitory synaptic activity in 80% of neurons, whereas excitatory synaptic activity was affected in less than 50% of neurons. In whole-cell current clamp recordings, brief somatic application of ACh induced cell-type specific responses in 79% of rat lamina II neurons, which included: depolarization and action potential firing, subthreshold membrane depolarization, biphasic responses characterized by transient depolarization followed by hyperpolarization and membrane hyperpolarization alone. Similar responses were seen in marmoset lamina II neurons and the properties of each neuron group were consistent across species. ACh-induced hyperpolarization was blocked by the muscarinic antagonist atropine and all forms of acetylcholine-induced depolarization were blocked by the nicotinic antagonist mecamylamine. The cholinergic system plays an important role in regulating nociception and this study contributes to our understanding of how circuit activity is controlled by ACh at a cellular level in primate and rodent spinal cord.

1. Introduction

Signals that alert us to painful stimuli are transmitted through nociceptive pathways from the periphery to the dorsal horn of the spinal cord and then to the brain. Interneurons within the superficial laminae (I-II) of the dorsal horn play a role in regulating nociceptive signals before they are transmitted further through the somatosensory system (Ribeiro-da-Silva and De Koninck, 2008). The activity of these neurons is modulated through a number of signalling pathways, including the cholinergic system (Naser and Kuner, 2017; Picciotto et al., 2012). Effects of the neurotransmitter acetylcholine (ACh) in the spinal dorsal horn are mediated through ionotropic nicotinic receptors (nAChRs) and metabotropic muscarinic receptors (mAChRs) (Coggeshall and Carlton, 1997; Hoglund and Baghdoyan, 1997; Stewart and Maxwell, 2003). Acetylcholine is released in the superficial laminae from cholinergic fibres that project from the deeper laminae of the dorsal horn forming a dense plexus of fibres in lamina I and II, as well as from the dorsal root ganglion (Bellier and Kimura, 2007; Mesnage et al., 2011). Lamina III

* Corresponding author. Department of Physiology, Monash University, Melbourne, VIC, 3800, Australia.
E-mail address: wendy.imlach@monash.edu (W.L. Imlach).

https://doi.org/10.1016/j.neuropharm.2021.108755
Received 14 April 2021; Received in revised form 8 August 2021; Accepted 10 August 2021
Available online 17 August 2021
0028-3908/© 2021 The Authors. Published by Elsevier Ltd. This is an open access article under the CC BY-NC-ND license (http://creativecommons.org/licenses/by-nc-nd/4.0/).

neurons also receive cholinergic input through descending projections from the brainstem (Stornetta et al., 2013), and nicotinic activation of brainstem nuclei is involved in driving spinal muscarinic activation (Iwamoto and Marion, 1993).

The cholinergic system has been shown to have an anti-nociceptive effect on signalling in the dorsal horn, where activation of nicotinic and muscarinic AChRs promote analgesia, as does increasing levels of endogenous spinal acetylcholine through acetylcholinesterase inhibition (Cucchiaro et al., 2008; Rashid and Ueda, 2002; Yoon et al., 2005; Aceto et al., 1986). Conversely, locally applied receptor antagonists can induce nociceptive mechanical hypersensitivity (Rashid and Ueda, 2002; Zhuo and Gebhart, 1991) and mechanical thresholds are under ACh-mediated tonic inhibitory control (Zhuo and Gebhart, 1991; Young et al., 2008; Rashid et al., 2006; Yalcin et al., 2011; Dhanasobhon et al., 2021). In humans, acetylcholinesterase inhibitors in particular have been successfully used as analgesics. Donepezil and neostigmine, which both act to increase levels of endogenous acetylcholine, are effective analgesics for migraine and post-surgical pain (Nicolodi et al., 2002; Lauretti et al., 1998). This anti-nociceptive role has highlighted the cholinergic pathway as a desirable target for the development of pharmacotherapies designed to treat pain (Naser and Kuner, 2017). However, the effects of cholinergic modulation do not all result in analgesia, as spinal administration of nicotinic acetylcholine agonists can also produce hyperalgesia *in vivo* (Genzen and McGehee, 2003; Khan et al., 1998), and different muscarinic ACh receptors have been shown to have opposing effects on GABA release in lamina II of the dorsal horn (Zhang et al., 2005), which makes the cellular and circuit activity of the dorsal horn in response to acetylcholine even more interesting.

Previous studies have shown that acetylcholine modulates nociceptive activity by increasing inhibitory signalling, with agonists of both muscarinic and nicotinic AChRs shown to increase glycinergic and GABAergic signalling in the superficial dorsal horn (Rashid and Ueda, 2002; Zhang et al., 2005; Kiyosawa et al., 2001; Wang et al., 2006; Laing et al., 1994; Baba et al., 1998). In a study by Cordero-Erausquin et al. (2004), the nicotinic responses of inhibitory and excitatory neurons from multiple laminae within the deep dorsal horn of neonatal mice were mapped (Cordero-Erausquin et al., 2004). Excitatory and inhibitory neurons were analysed and a difference in receptor subunit composition between the two neuronal classes were found. Neurons from both groups responded to nicotine application, however attempts at classifying the neurons by physiological parameters, such as firing patterns, show no correlation with receptor subtype or response (Cordero-Erausquin et al., 2004).

Dorsal horn interneurons show high heterogeneity, but can be broadly grouped by morphology and action potential firing patterns (Todd, 2017; Graham et al., 2007; Grudt and Perl, 2002). Morphological classification is based on size, position and orientation of dendritic arbors into four groups including central, islet, radial and vertical neurons (Todd, 2017). These groups have been reported to express different neurotransmitters, with islet neurons being inhibitory, central neurons existing as a mixed population, vertical being mostly excitatory and radial neurons are likely to be excitatory (Yasaka et al., 2010). More recent studies have categorised dorsal horn neurons into 30 molecular subtypes based on single cell RNA sequencing, identifying unique gene clusters (Haring et al., 2018). As there is no obvious arrangement of neurons within the nociceptive regions of the dorsal horn, we have focussed on lamina II, which is an area innervated by *C*- and Aδ-nociceptive primary afferent neurons, where all neurons are thought to receive input from afferent neurons and both excitatory and inhibitory interneurons (Todd, 2010). Lamina II is a major termination zone for primary afferents and this region receives cholinergic input from the deeper laminae and dorsal roots (Bellier and Kimura, 2007; Mesnage et al., 2011; Todd, 2010). Although there are no selective markers for specific cell types in lamina II, with commonly used markers including PKC-γ, NPY, SP and PV labelling overlapping cell types, we are able to use morphology and firing types to broadly classify the rat and primate neuronal subtypes. In addition to this, we have further investigated a radial interneuron subtype in this study by targeting Tac1 positive neurons in the mouse spinal cord (Peirs et al., 2020; Dickie et al., 2019).

Dorsal horn interneuron subtypes are thought to have distinct roles in regulating nociceptive transmission, however their cell-type specific responses to acetylcholine remains largely unexplored. Here, we sought to characterize how the different classes of interneuron respond to acetylcholine, classifying them by both morphology and firing type. We investigated the actions of acetylcholine on inhibitory and excitatory post-synaptic currents and membrane potential. Additionally, given reports of species-specific differences (Chen et al., 2010; Zhang et al., 2007) we also characterised the actions of acetylcholine on post-synaptic membrane potential changes in marmoset dorsal horn interneurons thus increasing translatability of results through to humans. Ultimately, increasing our understanding of how individual neurons respond to cholinergic modulation will increase our understanding of pain transmission as a whole, and may lead to identification of dysfunction during pain pathologies.

2. Materials and methods

2.1. Animals

Rat spinal cord tissue was used from adult male and female Sprague-Dawley rats (n = 48, 23 male and 25 female) aged between 8 and 16 weeks at the time of recording. For identification of Tac1 positive neurons in the mouse dorsal horn, a Tac1-IRES2-Cre-D mouse line (Jax stock # 021877) (Harris et al., 2014) was crossed with the Ai9 CAG promoter-driven tdTomato line (Jax stock # 007909) (Madisen et al., 2010). Spinal cord from male and female offspring, referred to as Tac1-TdTomato mice, aged between 16 and 24 weeks were used for experiments (n = 11, 6 male and 5 female). All rodents were housed in group cages on a 12 h/12 h light-dark cycle, at 22 °C with constant humidity. Rats and mice were anaesthetized with isoflurane and decapitated immediately prior to removal of the lumbar spinal cord in preparation for electrophysiology experiments. Marmoset spinal cord were scavenged from male and female adult *Callithrix jacchus* marmosets (n = 3, 2 male and 1 female), aged between 4 and 5.5 years that were anaesthetized with sufentanil for other experimental purposes. Prior to spinal cord removal, marmosets were euthanized by intravenous injection of sodium pentobarbital followed by transcardial perfusion of cold artificial cerebrospinal fluid (ACSF). All animal care and experimentation performed at Monash University was approved by the institutional animal ethics committee (Protocol number MARP/2017/062, for rodent studies).

2.2. Spinal slice preparation

The lumbar section of the spinal cord was exposed by laminectomy, removed and immersed in ice cold (0–4 °C) sucrose-based ACSF (mM): 100 sucrose, 63 NaCl, 2.5 KCl, 1.2 NaH2PO4, 1.2 MgCl2, 25 glucose and 25 NaHCO3. Parasagittal sections (340 μm) were cut using a vibratome (Leica VT1200s) and incubated for 15 min at 36 °C in NMDG-based recovery ACSF composed of (mM): 93 NMDG, 2.5 KCl, 1.2 NaH2PO4, 30 NaHCO3, 20 HEPES, 25 glucose, 5 sodium ascorbate, 2 thiourea, 3 sodium pyruvate, 10 MgSO4, and 0.5 CaCl2 adjusted to pH 7.4 with HCl. Slices were then transferred to ACSF composed of (mM): 125 NaCl, 2.5 KCl, 1.25 NaH2PO4, 1.2 MgCl2, 2.5 CaCl2, 25 glucose and 11 NaHCO3 for 45 min at 36 °C and then maintained at room temperature prior to transfer to the recording chamber. All ACSF solutions were equilibrated with 95% O2/5% CO2.

2.3. Electrophysiology

Slices were transferred to the recording chamber and continuously superfused with room temperature ACSF equilibrated with 95% O2/5%

CO2 at a rate of 2 ml/min. Dodt-contrast optics were used to identify lamina II neurons in the translucent substantia gelatinosa layer of the superficial dorsal horn. Tac1 positive neurons from Tac1-TdTomato mice were identified by their expression of red fluorescent protein in the substantia gelatinosa layer of the dorsal horn. Neurons were filled with Lucifer yellow and biocytin to allow identification of morphology and position at the end of the recording and subsequent post-hoc characterization of neuron morphology in fixed tissue. *Inhibitory post-synaptic current recordings:* Spontaneous inhibitory post-synaptic currents (sIPSCs) were recorded in whole-cell voltage clamp, held at −65 mV (not corrected for the liquid junction potential of 4 mV) with a CsCl based internal solution composed of (mM): 140 CsCl, 10 EGTA, 5 HEPES, 2 $CaCl_2$, 2 MgATP, 0.3 NaGTP, 5 QX-314.Cl, 2 Lucifer Yellow CH dipotassium salt and 0.1% biocytin (osmolarity 285–295 mosmol l−1). Patch clamp electrodes had resistances of 3–5 MΩ and ASCF contained NBQX (10 μM), AP5 (100 μM) to inhibit EPSCs. Baseline activity was recorded for a minimum of 2 min followed by 2 min of ACh superfusion (100 μM in ACSF). *Excitatory post-synaptic current recordings:* Spontaneous excitatory post-synaptic currents (sEPSCs) were recorded in whole-cell voltage clamp, held within the range of −35 to −50mV (adjusted for each neuron to eliminate sIPSCs) (Takeda et al., 2003), using a potassium gluconate based internal solution composed of (mM): 135 K gluconate, 10 HEPES, 0.5 EGTA, 8 NaCl, 2 MgATP, 0.3 NaGTP, 5 QX-314. Cl, 2 Lucifer Yellow CH dipotassium salt, 0.1% biocytin (osmolarity 285–295 mOsmol l-1). Patch clamp electrodes had resistances of 6–9 MΩ. Since nACh receptors are inhibited by the glycine and GABA antagonists strychnine, picrotoxin and bicuculline, these antagonists were not used in sEPSC experiments (Garcia-Colunga and Miledi, 1999; Matsubayashi et al., 1998; Demuro et al., 2001). Baseline activity was recorded for a minimum of 2 min followed by 2 min of ACh superfusion (100 μM in ACSF). Responding neurons were defined as those that changed by > 0.5x of baseline for synaptic frequency, or >10 pA for inward current amplitude. *Intrinsic activity:* Neuronal responses to ACh were recorded in whole-cell current clamp using a potassium gluconate based internal solution. Slices were superfused with normal oxygenated ACSF and patch clamp electrodes had resistances of 6–9 MΩ. Neuronal firing patterns were recorded in response to injection of depolarizing current steps using a range that induced an output of −100 mV increasing in 10–20 pA increments until at least two steps above rheobase. Brief pulses of ACh were applied through somatic application via pressure-pulse delivery (ACh 1 mM in ACSF; 4–6 psi for 30 ms), to determine single-cell responses. Fast somatic delivery was achieved using a large patch clamp electrode approximately 20–30 μm from the neuron soma. Three pulses were applied at a frequency of 0.1 Hz, repeated three times. A higher concentration of ACh was required for pulsed somatic application compared to bath applied ACh because of the rapid application and small volume. In a subset of recordings, mecamylamine (10 μM) and atropine (1 μM) were superfused into the slice chamber for at least 3 min prior to a second series of ACh puffs to determine whether nicotinic or muscarinic AChR were mediating the observed response. Morphology was determined at the end of each recording using Lucifer yellow fluorescence *in situ* while the patch pipette was in place, to avoid distorting the morphology by pulling the neurons from its original position. This allowed a real-time, rapid methodology to enable cells to be identified morphologically whilst undertaking the electrophysiological study, without need for post-hoc imaging and detailed analysis. The morphological criteria for islet and central cells include rostrocaudal dendrites that are long with many branches for islet neurons or few that are medium in length for central neurons. The dendrites of the vertical cells projected ventrally and radial cells had dendrites in all directions.

2.4. Histochemical staining for visualisation of patched neurons by confocal microscopy

At the end of electrophysiological recording, some slices from rat spinal cord that had intact neurons after the patch pipette had been removed were fixed in 4% paraformaldehyde in 0.1 M phosphate buffer (PB) composed of (M): 0.019 $NaH_2PO_4 \cdot 2H_2O$ and 0.081 Na_2HPO_4, pH 7.4, then washed in 0.1 M PB. Slices were incubated in 0.3% triton X-100 in 0.1 M PB for 4 h at room temp on a benchtop shaker, before incubation in a blocking solution (0.3% triton X, 1% bovine serum albumin (BSA), 5% horse serum) for 1 h. Slices were incubated for 2–3 h at room temperature with Alexa Fluor 488-conjugated streptavidin (Sigma) diluted in 1% BSA and 0.3% Triton X-100 in 0.1 M PB to stain biocytin-filled cells. Slices were washed in 0.1 M PB, mounted in ProLong Gold antifade reagent (Invitrogen) and imaged using confocal microscopy (Nikon C1 Inverted).

2.5. Drugs and chemicals

NBQX, D-APV, mecamylamine and atropine were purchased from Sapphire Bioscience, Australia, and acetylcholine chloride was purchased from Sigma Australia. QX-314 was purchased from Alomone Labs, Israel. All other chemicals were purchased from Sigma Australia unless otherwise stated.

2.6. Data acquisition and analysis

Electrophysiological data was acquired using a Sutter integrated Patch Clamp Amplifier (IPA) (Sutter Instrument, California) and recorded using SutterPatch running on Igor Pro 7 (WaveMetrics, Oregon) or a Multiclamp 700 B Amplifier (Molecular Devices, California) using Axograph X data acquisition software. Both voltage clamp and current clamp recordings were sampled at 10 kHz and stored for later offline analysis. All electrophysiological data was analysed in SutterPatch or Axograph X. Grouped data is presented, as mean ± standard error of the mean (SEM).

2.7. Statistical analysis

ACh-induced changes in post-synaptic current frequency, amplitude and inward current were compared to baseline using a Wilcoxon matched-pairs signed rank test on raw data. Differences in ACh responses between groups were compared using a Kruskal-Wallis test with Dunn's multiple comparisons test and differences between groups of each species were compared using a Kruskal-Wallis test with Dunn's multiple comparisons test. Differences in neuronal responses between morphological groups were determined using a Fisher's exact test, or a Chi-square test.

3. Results

3.1. Acetylcholine-induced differential modulation of the frequency of spontaneous synaptic currents in a cell-type specific manner

Whole-cell voltage-clamp recordings from 105 neurons from lamina II of the dorsal horn of naïve adult rats, showed that bath applied ACh (100 μM) increased, decreased or had no effect on spontaneous synaptic current activity in a cell-type specific manner. ACh affected inhibitory synaptic activity in 76% of neurons (n = 38/50), whereas excitatory synaptic activity was only changed in 30.9% of neurons (n = 17/55) (Fig. 1, Table 1).

Recordings of spontaneous inhibitory synaptic activity showed four response types, which included: an increase in sIPSC frequency (16 neurons, 32% of total); activation of an inward current with no change in IPSC frequency (2 neurons, 4% of total), a combined activation of an inward current and increase in sIPSC frequency (14 neurons, 28% of total); a decrease in sIPSC frequency (8 neurons, 16% of total), with the remaining 10 neurons (20% of total) showing no change in sIPSC activity or inward current in the presence of ACh (Fig. 1C and D, Table 1).

Cells were grouped into four morphological categories based on

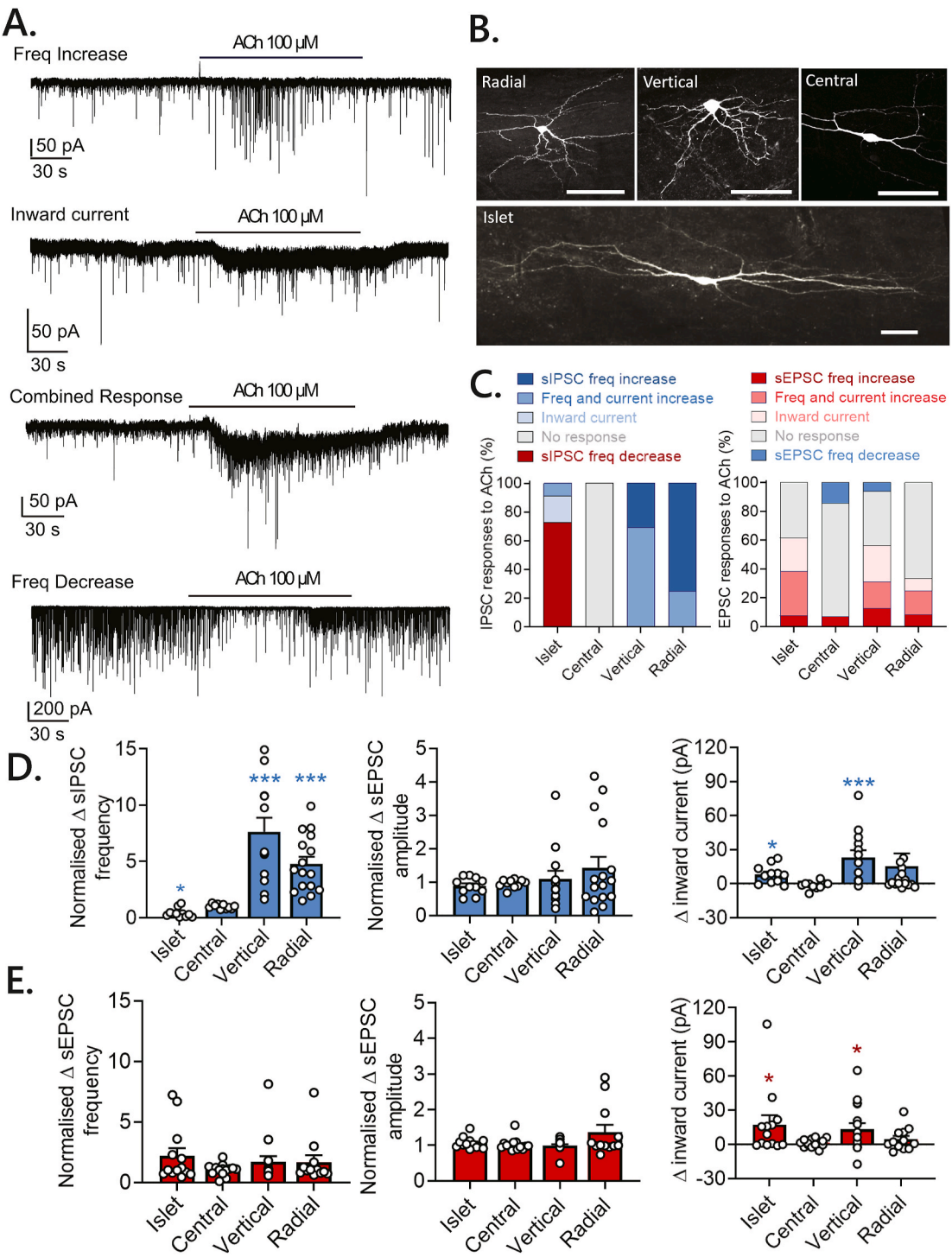


Fig. 1. Effects of ACh on spontaneous synaptic currents in rat dorsal horn interneurons. (a) Representative traces showing four different responses to 100 µM bath-applied acetylcholine recorded in voltage-clamp, which include an increase in spontaneous post-synaptic current frequency, an activation of an inward current, a combined activation of inward current and increase in spontaneous current frequency and a decrease in spontaneous postsynaptic current frequency. (b) Representative images of each of the lamina II interneuron types, imaged by confocal microscopy in biocytin filled neurons. Dorsal direction is up. Scale bar = 50 µm. (c) Proportion of inhibitory and excitatory response types to ACh in subsets of lamina II interneurons. IPSC responses (left) for islet (n = 11), central (n = 10), vertical (n = 13) and radial (n = 16) neurons. EPSC responses (right) for islet (n = 13), central (n = 14), vertical (n = 16) and radial (n = 12) neurons. Inhibitory responses are shown in blue shades, excitatory in red. (d) sIPSC frequency and amplitude normalized to baseline and change in inward current from baseline for each neuron group (*<0.05, ***<0.001, Wilcoxon matched-pairs signed rank test). (e) sEPSC frequency and amplitude normalized to baseline and change in inward current from baseline for each neuron group. Data is shown as mean ± SEM.

Table 1
Inhibitory and excitatory spontaneous postsynaptic current responses of each morphological group in response to ACh.

Morphological group (50 neurons)	Inhibitory post-synaptic current responses to ACh (% of total)				
	sIPSC frequency increase	Frequency increase and inward current	Inward current	No response	sIPSC frequency decrease
Islet (n = 11)	–	1 (9.1%)	2 (18.1%)	–	8 (72.7%)
Central (n = 10)	–	–	–	10 (100.0%)	–
Vertical (n = 13)	4 (30.8%)	9 (69.2%)	–	–	–
Radial (n = 16)	12 (75.0%)	4 (25.0%)	–	–	–
Morphological group (55 neurons)	Excitatory post-synaptic current responses to ACh (% of total)				
	sEPSC frequency increase	Frequency increase and inward current	Inward current	No response	sEPSC frequency decrease
Islet (n = 13)	1 (7.7%)	4 (30.7%)	3 (23.1%)	5 (38.5%)	–
Central (n = 14)	1 (7.1%)	–	–	11 (78.6%)	2 (14.3%)
Vertical (n = 16)	2 (12.5%)	3 (18.8%)	4 (25.0%)	6 (37.5%)	1 (6.3%)
Radial (n = 12)	1 (8.3%)	2 (16.6%)	1 (8.3%)	8 (66.7%)	–

previous descriptions, which included radial, vertical, central and islet interneurons (Grudt and Perl, 2002). Morphological criteria for islet and central cells include rostrocaudal dendrites with many long or very few medium in length, respectively, vertical cells had ventrally projecting dendrites and radial cells had dendrites in all directions. Morphology was determined at the end of each recording using Lucifer yellow fluorescence *in situ*, which was confirmed post hoc with biocytin-streptavidin staining in neurons that could be recovered (Imlach et al., 2016). Neurons with incomplete Lucifer yellow fills, or dendrites that were cut in a way that impeded morphological characterization, or atypical morphologies were excluded from analysis. There were 18 neurons of 68 recorded that were excluded from the IPSC data analysis (26.5%) and 11 neurons from 66 recordings excluded from the EPSC data analysis (16.6%). Although there was some overlap in responses across neuron subtypes, there were clear differences in the effects on inhibitory synaptic activity between groups (Fig. 1C and D, Table 1). The islet neurons were the only group to show a reduction in IPSC frequency in response to ACh (n = 8/11, 72.7%) with only one showing an ACh-induced increase in spontaneous currents (9.1%). All central neurons (n = 10/10) showed no response to ACh either in terms of changes in spontaneous IPSCs or activation of an inward current response to ACh. All vertical and radial neurons showed an increase in frequency of IPSCs or a combination of increased frequency and activation of an inward current. The sIPSC frequency was significantly increased in both of these neuron groups (Wilcoxon test, vertical W = 91, p = 0.0002; radial W = 136, p=<0.0001) and ACh-induced inward current was apparent in the vertical neurons (Wilcoxon test, W = −89, P = 0.0005) and islet neurons (W = −58, P = 0.007). Spontaneous IPSC amplitude was not significantly different in the presence of ACh in any of the neuron groups (Fig. 1D). Statistical difference between baseline and ACh response was determined using a Wilcoxon matched-pairs signed rank test on non-normalized data. Overall, ACh increased inhibitory synaptic input onto these excitatory neuron subtypes (radial and vertical neurons), while decreasing inhibitory input to most of the inhibitory islet neurons, leaving central neurons as the only non-responsive cell type.

Recordings of excitatory synaptic activity showed four response types, which include an increase in sEPSC frequency (5 neurons, 9.1% of total), activation of an inward current with no change in sEPSC frequency (8 neurons, 14.5% of total), a combined activation of an inward current and increase in sEPSC frequency (9 neurons, 16.3% of total) and a decrease in sEPSC frequency (3 neurons, 5.4% of total), with the remaining 30 neurons (54.5% of total) showing no change in sEPSC activity or inward current in the presence of ACh (Fig. 1C,E, Table 1). There were fewer responding neurons in the excitatory postsynaptic current group and the responses across neuronal subtypes were less well defined. There was no significant difference in sEPSC frequency or amplitude but there were significant differences in the inward current in response to ACh in the vertical neurons (Wilcoxon signed rank test, W = −82, P = 0.03) and islet neurons (W = −71, P = 0.01) (Fig. 1E). A Chi-square test showed no significant difference between groups when numbers of responding neurons were compared to those that did not respond, $X^2(3, N = 55) = 1.458$, p = 0.69. No difference was observed between morphologies or responses to ACh in male and female spinal cord.

3.2. Membrane potential responses of lamina II interneurons to brief somatic application of acetylcholine

Membrane potential responses to pressure pulse application of ACh (1 mM) applied directly to the soma of laminal II interneurons for 30 ms (3–6 psi) were recorded in whole-cell current clamp mode from a total of 76 neurons from adult rat dorsal horn. Four distinct changes in postsynaptic membrane properties were observed characterized by: changes in action potential (AP) firing rate (n = 25/76, 32.9%); a transient, membrane depolarization that failed to reach threshold for action potential firing (n = 22/76, 28.9%); a biphasic membrane depolarization followed by a transient membrane potential hyperpolarization (n = 5/76, 6.6%); a transient membrane potential inhibition and hyperpolarization alone (8/76, 10.5%), with no response observed in 16/76 neurons (21.0%) (Fig. 2A). Responses differed between neuronal subtypes, with most radial neurons responding to ACh with transient membrane depolarization (n = 10/11, 90.9%) and islet neurons responding with action potential firing (n = 12/15, 80.0%) or transient membrane depolarization (n = 3/15, 20%). Half of the central neurons tested did not respond to somatic ACh application (n = 10/20, 50.0%), whilst the remainder responded with membrane potential hyperpolarization (n = 3/20, 15%) or depolarization (n = 6/20, 30%). A Chi-square test showed a significant difference in response to ACh between morphological groups $X^2(12, N = 76) = 52.21$, p < 0.0001. There were 26 neurons of 102 recorded (25.5%) with atypical or unclear morphology that were excluded from the membrane potential response data as they could not be classified into any of the 4 morphological groups. Responses in vertical neurons were heterogeneous, with all ACh response types observed in this neuronal class (Fig. 2B). There was no significant difference in resting membrane potential between neuronal subtypes, but rheobase was found to be significantly higher in central neurons compared to compared to islet neurons (P = 0.0055) cell types. Significance was determined using a Kruskal-Wallis test with Dunn's multiple comparisons test (Table 2).

In addition to grouping by morphology, lamina II interneurons were also grouped by firing type, using a system previously described for dorsal horn interneurons (Balachandar and Prescott, 2018). When neurons were grouped by characteristic firing properties (Fig. 2D), including delayed (n = 11), single spike (n = 19), phasic (n = 11), gap (n = 9) and tonic (n = 26), the responses to ACh were less well defined. All groups included neurons that responded with action potentials except the delayed firing group and all but the tonic firing group had neurons in which ACh induced membrane potential hyperpolarization (Fig. 2C). Resting membrane potential was not significantly different between

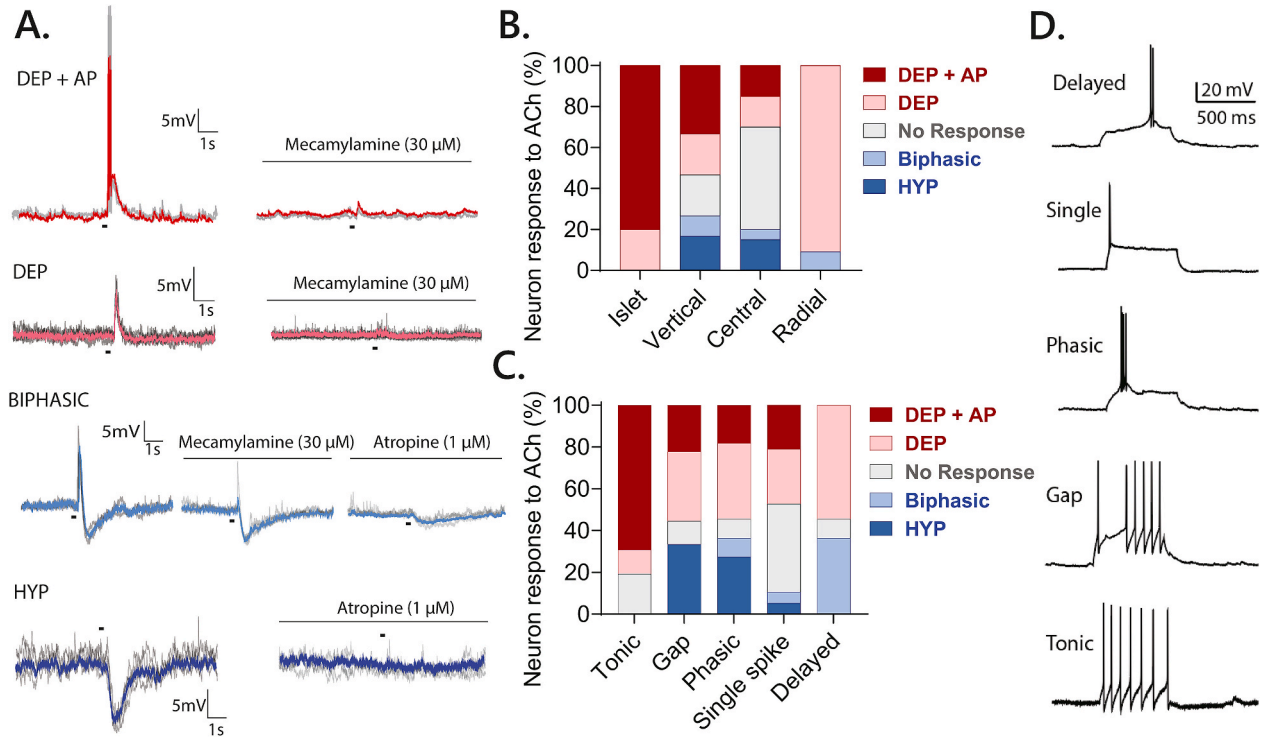


Fig. 2. Effect of ACh on membrane potential responses of rat dorsal horn interneurons. (a) Left: Representative traces showing responses of lamina II interneurons to ACh pulses (1 mM, 30 ms), indicated by the short black bars recorded in whole-cell current clamp. Raw traces are shown in grey (lighter in background), with average traces in colour (darker in foreground). DEP + AP, Depolarization + action potential; DEP, depolarization; HYP, hyperpolarization. Right: Responses to ACh responses following incubation with the nAChR antagonist mecamylamine or the mAChR antagonist atropine. (b) Proportion ACh responses grouped by lamina II interneuron type, including radial (n = 11), central (n = 20), vertical (n = 30) and islet (n = 15) neurons. (c), Proportion ACh responses grouped by firing type, including delayed firing (n = 11), single spike (n = 19), phasic (n = 11), gap (n = 9), tonic (n = 26) (d), Representative traces of the firing types used to classify neurons.

Table 2
ACh responses of rat dorsal horn interneuron subtypes grouped by morphology. Rat lamina II interneuron responses to brief somatic application of ACh (1 mM, 30 ms) recorded in whole-cell current-clamp. Cells were classified by morphology based on Lucifer Yellow filling *in situ*.

Neuron group (76 neurons)	Response to ACh (% of cells)					Intrinsic properties	
	Depolarization + AP	Depolarization	No response	Biphasic	Hyperpolarization	RMP (mV)	Rheobase (pA)
Radial (n = 11)	–	10 (90.9%)	–	1 (9.1%)	–	−65.1 ± 1.9	33.6 ± 4.8
Central (n = 20)	3 (15.0%)	3 (15.0%)	10 (50.0%)	1 (5.0%)	3 (15.0%)	−61.7 ± 2.5	70.7 ± 10.2
Vertical (n = 30)	10 (33.3)	6 (20.0%)	6 (20.0%)	3 (10.0%)	5 (16.7%)	−61.4 ± 1.4	39.0 ± 4.9
Islet (n = 15)	12 (80.0%)	3 (20.0%)	–	–	–	−58.3 ± 1.5	28.6 ± 4.9

groups. However, there were differences in rheobase between tonic firing neurons and other groups, with significantly higher rheobase in single spike neurons (Kruskal-Wallis test, H = 28.33, df = 4, P < 0.0001), delayed neurons (P = 0.018) and gap firing neurons (P = 0.0069), with no significant difference in rheobase between other firing types (Table 3). Significance was determined using a Kruskal-Wallis test with Dunn's multiple comparisons test. A Chi-square test showed no significant difference between groups based on firing type when numbers of responding neurons were compared to those that did not respond $X^2(4, N = 76) = 4.178$, p = 0.38.

3.3. Responses of lamina II interneurons correspond to nicotinic or muscarinic receptor activation

To determine whether the membrane potential responses recorded in lamina II interneurons were due to activation of muscarinic or nicotinic

Table 3
ACh responses of rat dorsal horn interneuron subtypes grouped by action potential firing. Rat lamina II interneuron responses to brief somatic application of ACh (1 mM) recorded in whole-cell current-clamp. Cells were classified by firing pattern in response to current injection.

Firing type (76 neurons)	Responses (% of total)					Intrinsic properties	
	Depol + AP	Depol	No response	Biphasic	Hyperpol	RMP (mV)	Rheobase (pA)
Delayed (n = 11)	–	6 (54.5%)	1 (9.1%)	4 (36.4%)	–	−66.1 ± 1.7	48.7 ± 6.4
Single spike (n = 19)	4 (21.1%)	5 (26.3%)	8 (42.1%)	1 (5.3%)	1 (5.3%)	−59.3 ± 2.3	73.3 ± 11.4
Phasic (n = 11)	2 (18.2%)	4 (36.4%)	1 (9.1%)	1 (9.1%)	3 (27.3%)	−63.0 ± 1.7	40.0 ± 8.9
Gap (n = 9)	2 (22.2%)	3 (33.3%)	1 (11.1%)	–	3 (33.3%)	−68.1 ± 3.3	61.1 ± 13.3
Tonic (n = 26)	18 (69.2%)	3 (11.5%)	5 (19.2%)	–	–	−59.7 ± 1.4	21.0 ± 2.4

acetylcholine receptors, the effects of bath application of the nAChR antagonist mecamylamine (30 μM) or mAChR antagonist atropine (1 μM) were tested on ACh-induced responses. ACh-induced excitatory responses including depolarization and suprathreshold depolarization were abolished in the presence of mecamylamine (13/13 neurons), which suggests that neuronal activation and excitation by ACh was nAChR-dependent. Conversely, membrane potential hyperpolarization and inhibitory responses induced by ACh were abolished in the presence of atropine (5/5 neurons), which suggests that inhibition and membrane potential hyperpolarization was mAChR-dependent. In neurons characterized by biphasic shifts in membrane potential induced by ACh, transient membrane potential depolarization was blocked in the presence of mecamylamine whilst ACh-induced hyperpolarization persisted, an effect which was then attenuated by atropine (Fig. 2A). No differences in cell-type responses were observed in neurons from male and female rats.

3.4. ACh-induced responses in Tac1 positive lamina II mouse interneurons

A recent study by Dickie et al. (2019) showed that many cells that express substance P, encoded by *Tac1*, are radial in morphology (Dickie et al., 2019). To investigate whether this subset of radial neurons had similar response types to ACh as the radial interneurons from rat spinal cord, we recorded from radial neurons that were Tac1 positive in the dorsal horn of Tac1-TdTomato mice. In these mice, TdTomato is present in all adult neurons that have expressed Tac1 at any stage of development, which may include neurons that no longer express substance P (Gutierrez-Mecinas et al., 2017). To ensure only Tac1 expressing radial neurons were included in the analysis, neurons were filled with Lucifer Yellow and morphology determined at the end of the recording *in situ*. There were 4 Tac1 positive neurons of 36 recorded (10.0%) where morphology could not be determined at the end of recording and these were excluded from the data analysis. From the remaining 32 neurons where morphology could be determined, 24 had radial morphology and the remaining 8 neurons had central interneuron morphology. Only those with radial morphology were used for analysis. Firing patterns were recorded in experiments examining somatic application of ACh and bath applied ACh for the EPSC response experiments (n = 16) and of these neurons, 10 had delayed firing (68.8%) (Fig. 3D), 3 had single firing (18.8%) and 2 had initial firing that subsided (12.5%). The proportion of delayed firing neurons was similar to what we observed in rat radial neurons from the somatic ACh application experiment, where 9/11 cells (81.8%) had delayed firing and 2/11 cells (18.2%) had single spike firing and a Chi-square test showed no significant difference between firing types of rat radial neurons and mouse Tac1 neurons $X^2(2, N = 26) = 1.677$, $p = 0.432$.

Whole-cell voltage-clamp recordings from 16 Tac1 positive radial neurons from lamina II of the dorsal horn of naïve adult mice, showed that bath applied ACh (100 μM) increased sIPSC frequency in 100% of neurons (n = 8/8), with an increase in inward current in one of these neurons (n = 1/8, 12.5%). These results were very similar to those observed in radial neurons from rat dorsal horn (Fig. 3A and B), however the increase in sIPSC frequency was significantly higher in rat radial neurons (P = 0.010, unpaired, two-tailed Mann-Whitney test). The sIPSC amplitude only increased in one Tac-1 positive neuron and the effects of ACh on sIPSC and sEPSC amplitude and inward currents were not significantly different to responses recorded from rat radial neurons (P = 0.83, P = 0.96, respectively) (Fig. 3A). Bath applied ACh (100 μM) had no effect on EPSC frequency, amplitude or inward current in 100% of Tac1 positive neurons (n = 8/8), and were not significantly different to rat radial neuron responses (P = 0.57, P = 0.20, P = 0.48, respectively, unpaired, two-tailed Mann-Whitney test).

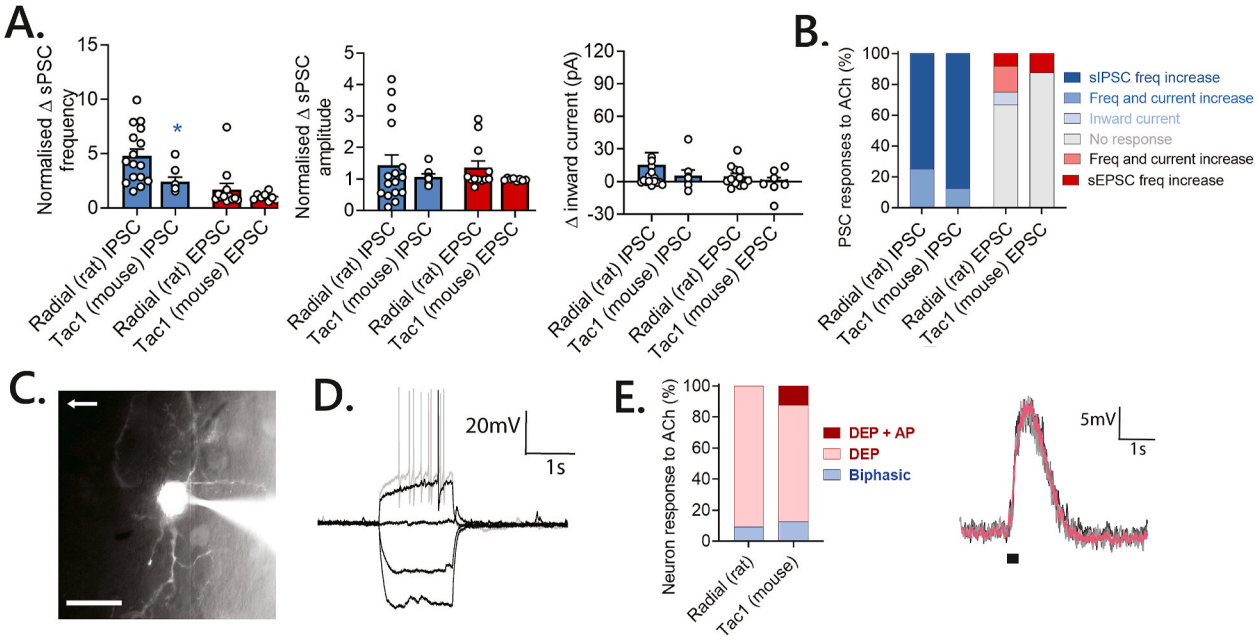


Fig. 3. Effects of ACh on Tac1-TdTomato positive radial neurons in lamina II of the mouse dorsal horn, compared to rat radial lamina II neurons. (a) Changes in inhibitory and excitatory postsynaptic currents in rat radial neurons and mouse Tac1 positive interneurons in response to bath-applied ACh (100 μM). Changes in the IPSC frequency and amplitude and inward current (blue bars) in response to ACh recorded from rat radial neurons (n = 16) and Tac1 positive radial neurons (n = 8) and EPSC frequency and amplitude and inward current (red bars) in response to ACh recorded from rat radial neurons (n = 12) and Tac1 positive radial neurons (n = 8). The PSC frequency and amplitude normalized to baseline and change in inward current from baseline is shown for each neuron group (*<0.05, Mann-Whitney test). (b). Proportion of inhibitory and excitatory response types to ACh in rat radial interneurons and Tac1 positive mouse radial interneurons. (c) Image of a mouse Tac1 positive radial neuron with Lucifer yellow fluorescence at the end of recording *in situ*. Scale bar = 20 μm. Arrow indicates dorsal direction (d) Representative example of a Tac1 positive radial membrane potential responses to current steps. (e) Proportion membrane potential responses of rat radial neurons and Tac1 positive mouse radial neurons to brief somatic application of ACh (1 mM), DEP + AP, Depolarization + action potential; DEP, depolarization, Biphasic, both EPSC and IPSC response. Trace shows neuron responses to brief somatic application to ACh pulses (1 mM, 30 ms), indicated by the short black bars recorded in whole-cell current clamp. Raw traces are shown in grey (lighter in background), with average traces in red (in foreground).

Membrane potential responses to pressure pulse application of ACh (1 mM) applied directly to the soma of Tac1 positive radial neurons for 30 ms (3–6 psi) were recorded in whole-cell current clamp mode from a total of 8 neurons from adult mouse dorsal horn. Three distinct changes in post-synaptic membrane properties were observed characterized by: depolarization and action potential (AP) firing (n = 1/8, 12.5%); a transient, membrane depolarization that failed to reach threshold for action potential firing (n = 6/8, 75.0%) and a biphasic membrane depolarization followed by a transient membrane potential hyperpolarization (n = 1/8, 12.5%) (Fig. 3E). A Fisher's exact test showed no significant difference between Tac1 positive radial neurons and radial neurons from rat dorsal horn (P > 0.999). For this test the AP+Depol data group was combined with the Depol group.

3.5. ACh-induced responses in marmoset dorsal horn lamina II interneurons: comparison to effects in rodents

To determine whether lamina II interneurons within nociceptive circuits of the primate spinal cord had similar ACh responses to those observed in rodent neurons, we performed whole-cell current clamp recordings on 30 neurons from marmoset dorsal horn. Similar responses to ACh were observed including depolarization associated with action potential firing (8/30 neurons, 26.7%), transient depolarization (9/30 neurons, 30.0%), transient membrane potential hyperpolarization (4/30 neurons, 13.3%) with no response observed in 9/30 neurons (30%). The ACh-induced biphasic transient depolarization followed by membrane potential hyperpolarization reported in rat spinal cord was not observed in any of the recorded neurons. However, as the frequency of this biphasic response was low in rat dorsal horn (5.2%), the relatively smaller population of dorsal horn neurons recorded from marmoset in the present study may account for this difference.

Marmoset lamina II interneurons were grouped by morphology into radial (n = 8), central (n = 11), vertical (n = 5) and islet (n = 7) groups, which showed similar responses to the equivalent morphological groups characterized in rat (Table 4). All radial neurons responded to ACh with a transient membrane potential depolarization, while the majority of central neurons did not respond (7/11, 63.6%) to ACh. ACh-induced responses in vertical neurons were mixed including depolarizing and hyperpolarizing responses and most islet neurons (5/6, 83.3%) responded to ACh with transient membrane potential depolarization sufficient to drive action potential firing, similar to rat islet neurons (Fig. 4C). There was no significant difference in resting membrane potential or rheobase between morphological groups in the marmoset (Kruskal-Wallis test with Dunn's multiple comparisons test). Resting membrane potential and rheobase values for rat and marmoset were similar and there was no significant difference between morphological groups from each species (Kruskal-Wallis test with Dunn's multiple comparisons test).

Marmoset neurons were also grouped by firing type and responses to ACh compared. There were no gap firing neurons recorded in this data set, likely due to the sample size, and there were only 2 delayed firing neurons which were combined with the phasic firing neurons for analysis (Fig. 4). Groups based on firing type showed similar responses to those from rat spinal cord, with a similar proportion of non-responding and ACh-induced transient membrane potential depolarization responding neurons in the single spike group, mixed responses in the phasic and delayed group and mostly ACh-induced depolarization and action potential firing in the tonic group (4/6 neurons, 66.7%). There were no significant differences in resting membrane potential between groups based on firing type from marmoset dorsal horn, but rheobase in single spike neurons was significantly higher than tonic firing neurons (H = 10.68, df = 2, P = 0.0054, Kruskal-Wallis test with Dunn's multiple comparisons test) (Table 5). Resting membrane potential and rheobase were not significantly different between each firing group from marmoset and rat (Kruskal-Wallis test with Dunn's multiple comparisons test). These results indicate that, for the main part, acetylcholine produces similar responses in marmoset dorsal horn interneurons to those observed in rodent models. A Chi-square test showed no significant difference between groups based on firing type when numbers of responding neurons were compared to those that did not respond $X^2(2, N = 30) = 1.481$, p = 0.48.

4. Discussion

The cholinergic system regulates nociceptive signaling in the dorsal horn via pre- and post-synaptic mechanisms. Cholinergic interneurons in the dorsal horn have been previously characterized based upon the morphology, neurochemistry and firing of these neurons from lamina III-IV of the mouse spinal cord (Mesnage et al., 2011). However, until now the postsynaptic neurons in the dorsal horn that receive and respond to cholinergic input have not been characterized or their responses described. Although there are no selective markers for specific cell types in the rodent spinal cord, we are able to use morphology and firing types to broadly classify the rat and primate neuronal subtypes (Peirs et al., 2020). Here we investigated the effects of ACh on pre- and postsynaptic membrane excitability in morphologically defined neuronal subsets of lamina II interneurons to provide insight of how cholinergic signaling integrates within the circuit and controls nociceptive output.

In order to understand how ACh affects inhibitory synaptic activity within the local nociceptive circuits in the spinal cord, we measured changes in spontaneous synaptic inhibitory currents over a range of neuronal subtypes in lamina II. We found that ACh increased inhibitory signaling onto excitatory radial and vertical neurons, which suggests that ACh functions to reduce excitability of these neurons, and as a consequence reduces nociceptive output. A study by Li et al. (2002) showed that the ACh-induced increase in GABA receptor mediated IPSC frequency in lamina II neurons is abolished by atropine, whilst a separate study by Takeda et al. (2003) showed that nicotine-induced increases in IPSC frequency is abolished by mecamylamine in lamina II (Takeda et al., 2003; Li et al., 2002). Taken together these data suggest ACh-induced effects on IPSC frequency is mediated through both muscarinic and nicotinic ACh receptors. Surprisingly, there was no ACh-induced change in inhibitory synaptic input to central neurons, even though basal levels of spontaneous inhibitory activity were similar to other neuronal types. Our previous studies have shown that these neurons, on average, receive similar levels of glycinergic and GABAergic synaptic input, which is not significantly different to the other neuronal subtypes, so we can rule out GABA or glycine specific effects (Imlach et al., 2016). These results suggest that the presynaptic inhibitory

Table 4
ACh responses of primate dorsal horn interneuron subtypes grouped by morphology. Marmoset lamina II interneuron responses to brief somatic application of ACh (1 mM, 30 ms) recorded in whole-cell current-clamp. Cells were classified by morphology based on Lucifer Yellow filling *in situ*.

Cell Type (30 neurons)	Responses of marmoset cells (% of total)					Intrinsic properties	
	Depol+AP	Depol	No response	Biphasic	Hyperpol	RMP (mV)	Rheobase (pA)
Radial (n = 8)	–	8 (100.0%)	–	–	–	−62.6 ± 2.6	50 ± 30.8
Central (n = 11)	1 (9.1%)	–	7 (63.6%)	–	3 (27.3%)	−58.4 ± 2.3	30.9 ± 4.9
Vertical (n = 5)	2 (40.0%)	–	2 (40.0%)	–	1 (20.0%)	−55.4 ± 2.3	24.0 ± 9.0
Islet (n = 6)	5 (83.3%)	1 (16.6%)	–	–	–	−58.2 ± 2.2	18.3 ± 3.3

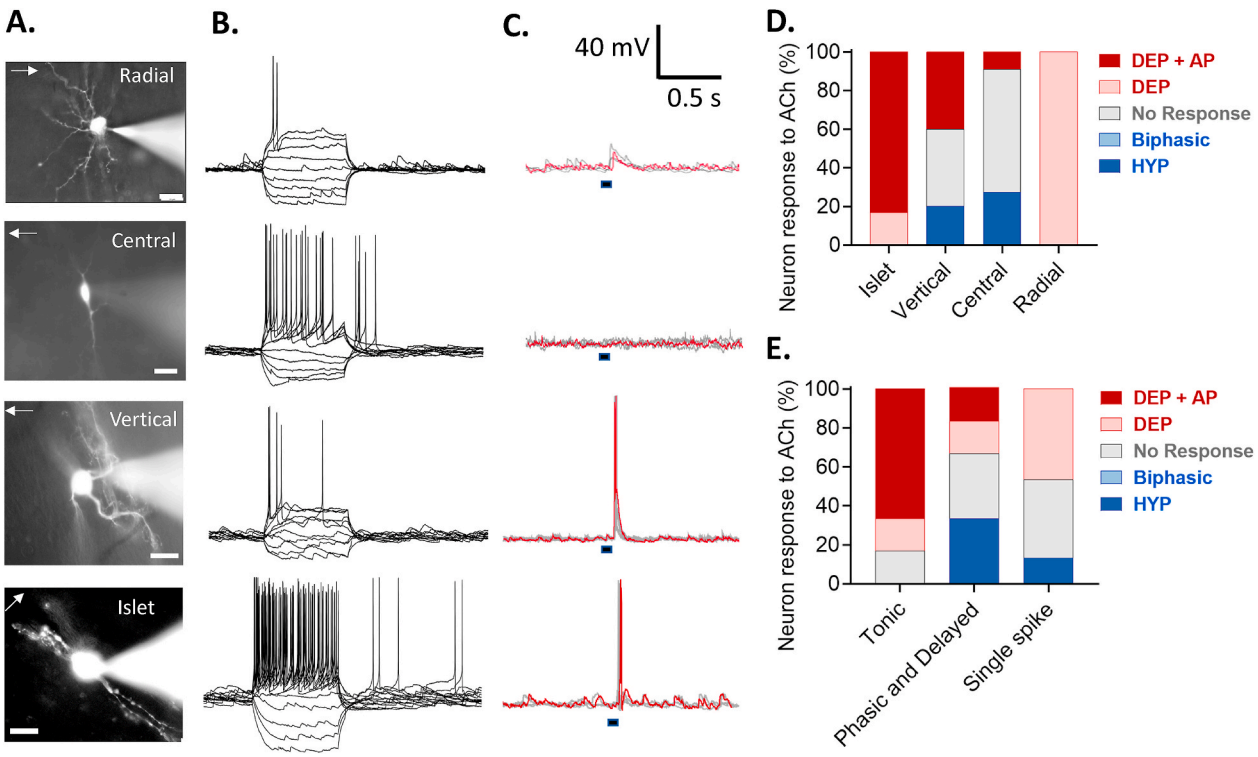


Fig. 4. Effect of ACh on marmoset dorsal horn interneurons. (a) Images of marmoset lamina II interneurons with Lucifer yellow fluorescence at the end of recording *in situ*. Arrows indicate dorsal direction. Scale bar = 20 μm. (b), Membrane potential responses to current steps showing firing types of each neuron. (c), Neuron responses to brief somatic application to ACh pulses (1 mM, 30 ms), indicated by the short black bars recorded in whole-cell current clamp. Raw traces are shown in grey (lighter in background), with average traces in red (darker in foreground). (d), Proportion ACh responses grouped by lamina II interneuron type, including radial (n = 8), central (n = 11), vertical (n = 5), and islet (n = 6) neurons. (e) Proportion ACh responses grouped by firing type, including single spike (n = 15), phasic or delayed (n = 9) and tonic (n = 6).

Table 5
ACh responses of primate dorsal horn interneuron subtypes grouped by action potential firing. Marmoset lamina II interneuron responses to brief somatic application of ACh (1 mM, 30 ms) recorded in whole-cell current-clamp. Cells were classified by firing pattern in response to current injection.

Cell Type (30 neurons)	Responses of marmoset cells (% of total)					Intrinsic properties	
	Depol+AP	Depol	No response	Biphasic	Hyperpol	RMP (mV)	Rheobase(pA)
Single spike(n = 15)	–	7(46.7%)	6(40.0%)	–	2(13.3%)	−59.9 ± 2.1	44.7 ± 8.1
Phasic/Delayed(n = 9)	4(66.6%)	1(16.6%)	2(33.3%)	–	2(33.3%)	−59.0 ± 1.9	23.3 ± 3.4
Tonic(n = 6)	4(66.7%)	1(16.7%)	1(16.7%)	–	–	−56.8 ± 2.4	15.0 ± 0.0

neurons that synapse with central interneurons are functionally and pharmacologically different to those in the radial and vertical circuits. Responses recorded from the inhibitory islet neuron group were the most interesting as the spontaneous inhibitory currents in the majority of these cells (72.7%) decreased in response to ACh. The effect of decreasing sIPSCs suggests that islet neuron activity could increase, as an indirect consequence or disinhibition, potentially reducing nociceptive output. The four morphological groups used in this study show clear differences in response to acetylcholine in relation to inhibitory activity and may contribute to our understanding of the nociceptive circuits involved in ACh-mediated analgesia (see graphical abstract). A previous study showed that nicotine increased sIPSC frequency in 86% of neurons in neonatal mouse spinal cord, across the whole dorsal horn. This is a higher percentage of neurons compared to our study where 30/50 neurons (60%) in lamina II of the dorsal horn had increased sIPSC frequency, which may be due to difference in the neurons across dorsal horn laminae, or may reflect network activity associated with neonatal development (Genzen and McGehee, 2005). However, a study by Takeda et al. (2003) found that activation of nACh receptors in the inhibitory presynaptic terminals in the substantia gelatinosa result in an increase the frequency of sIPSCs and mISPCs in 90% of neurons tested. This study showed that most nicotinic effects on inhibitory synaptic activity in substantia gelatinosa neurons were not associated with nicotine induced increases of excitatory glutamatergic activity (Takeda et al., 2003). We observed less effect of ACh on excitatory synaptic currents, with no groups showing significant differences in the presence of ACh, suggesting that the modulation of neuronal excitability by ACh is predominantly mediated through inhibitory signaling. Our results show an increase in sEPSC frequency in 14/55 neurons (25.5%) with a decrease in sEPSC frequency in 3/55 neurons (5.5%), which differs from Li et al. (2002), who previously showed an overall decrease in mEPSC frequency of 51.9 ± 2.4% in 13 neurons. One difference in our experiments is that we did not use antagonists for the $GABA_A$ and glycine receptors, while in the study by Li et al., they used bicuculine and strychnine, which have been shown to inhibit nAChR activation (Matsubayashi et al., 1998; Demuro et al., 2001). This suggests that the ACh effects on mEPSCs observed by Li et al., were entirely mediated by mAChR activation, which was confirmed in their experiments where they applied atropine and had no ACh-induced effect on mEPSC activity, while ACh was still able to reduce mEPSC frequency in the presence of mecamylamine (Li et al., 2002). In the current study, the sEPSC responses to ACh were mediated by the nAChR and the mAChR, resulting

in both frequency increases and decreases. It may be that the sEPSC increases in our experiments, could reduce the likelihood of measuring the sEPSC decreases that are driven by mAChR activation, which would lead to a lower number of neurons with sEPSC decreases. This may result in higher ratios of non-responding neurons (30/55 neurons, 54.5%), or those with increased frequency of sEPSCs (25.5%) (Fig. 1, Table 1). In future studies, this could be tested by repeating experiments under the current experimental conditions in the presence or atropine or mecamylamine. Experiments could also be repeated using the glycine receptor antagonist PMBA and the $GABA_AR$ antagonist gabazine, which are less likely to have an inhibitory effect on ACh receptors. However, the effect on preventing inhibitory or excitatory activity on network activity in these recordings must be taken into consideration, as the responses observed in the presence of synaptic receptor inhibitors will have an effect on all down/upstream synapses, not just those that are being investigated. For example, the study by Li et al. (2002) suggests that ACh inhibits glutamatergic synaptic inputs into lamina II neurons through presynaptic muscarinic and $GABA_B$ heteroreceptors, which may contribute to the antinociceptive action of ACh (Li et al., 2002).

We next investigated the effects of ACh on resting membrane potential of lamina II interneurons, where we found a neuronal subtype-dependent pattern of responses. Radial neurons depolarized in response to ACh, but not enough to reach threshold for action potential firing. Central and vertical neurons had mixed responses, with the majority of central neurons not responding. These two groups both had neurons that were hyperpolarized and activity reduced. Although neurons classified as central neurons are morphologically similar to each other, the group includes both inhibitory and excitatory interneurons and it may be that some of the inhibitory neurons are excited and excitatory neurons inhibited in this case. We have observed vertical neurons that can also be broken down into two morphological groups, including tap-like vertical neurons and umbrella shaped vertical neurons (data not shown), which may show differences, however these groups were not separated out in this current study. This may also contribute to the differences observed in the distribution of responses observed in voltage-clamp compared to the current clamp-experiments. Experiments in cesium-chloride loaded cells were specifically designed to facilitate observations of spontaneous IPSCs and are difficult to compare to responses observed in the current-clamp experiments. Voltage clamp experiments were undertaken with cesium chloride-based intracellular solutions at a holding potential of −65mV, conditions in which cesium would block most potassium channels and render chloride-mediated currents excitatory inward currents. Under these conditions we observed no inhibitory outward currents, unlike our studies in current clamp where clear membrane hyperpolarisations were observed. For example, 69.2% of neurons showed activation of an inward current and an increase in the frequency of sIPSC's (recorded as excitatory inward currents by chloride loading cells), while only 26.7% of vertical neurons show hyperpolarization, or a biphasic response in response to somatic application of ACh in current clamp-experiments. Several explanations may account for this. Firstly, the persistent inward currents activated by ACh in voltage-clamp may have been mediated via a number of other non-chloride-dependent mechanisms that contribute to the excitatory responses observed in current clamp, for example non-selective cation permeable TRP channels (Kichko et al., 2013). The increased frequency of ACh-induced sIPSCs generated by increased network activity in voltage-clamp experiments may also be driving the net inward current and this effect may be less obvious when only the somato-dendritic ACh receptors from a single neuron are activated in current-clamp experiments. It is also possible that in cesium-chloride-loaded cells other chloride-dependent mechanisms could contribute to the inward current, for example muscarinic receptor-dependent activation of calcium-activated chloride channels (Zhu et al., 2011). Alternatively, bath application of ACh may also desensitize some of the nAChR's, allowing the inward current driving mAChRs to appear more prominent. Further work is being undertaken to fully elaborate on the exact ionic mechanisms underlying the effects of ACh observed in this study.

Islet neurons were very different to other neuron groups as most responded to ACh with depolarization and action potential firing. Since these neurons are inhibitory activation would likely lead to an overall reduction in excitability. Differences in neuronal responses are most likely to reflect different ACh receptor expression, including subtypes of nAChR and mAChR. A study by Cordero-Erausquin et al. (2004) showed that both inhibitory and excitatory neurons throughout the dorsal horn of neonatal mice responded to nicotinic stimulation in voltage clamp recordings (73% of neurons), but the subtypes of nAChRs expressed by excitatory neurons (α3, β2 and α7) differed to those expressed by inhibitory neurons. In their study, neurons were grouped by firing pattern, but there was no correlation between firing type and nAChR markers observed (Cordero-Erausquin et al., 2004). Taking this study into consideration with our data that concentrates on lamina II neurons and still shows mixed responses over the firing type groups, may suggest that morphological groups provide a more reliable classification system than grouping of neurons based on firing patterns.

When we investigated whether different ACh responses corresponded to nicotinic or muscarinic receptor activation, we found that all of the depolarizing responses could be eliminated by a nicotinic receptor antagonist mecamylamine, while all of the ACh-induced hyperpolarizing responses could be abolished with the muscarinic receptor antagonist atropine. These results very clearly show the opposing roles of these two somatically expressed receptors in neuronal excitability. It is known that activating mAChRs reduces pain in rodents and humans and this study suggests that these inhibitory effects on local dorsal horn circuitry may be a contributing factor (Fiorino and Garcia-Guzman, 2012). Nicotinic agonists, which increase excitability, are also known to have analgesic effects, which has been reported to involve GABAergic transmission (Genzen and McGehee, 2005). Our data showing increased activity of inhibitory islet cells in response to ACh supports this, but it is less clear how the increased activity of radial neurons would affect circuit activity and overall output from dorsal horn circuits.

Behavioural studies by Chiari et al. (1999), and Lavand'homme and Eisenach (1999), have shown sex differences in cholinergic analgesia in thermal pain and mechanical allodynia, where intrathecal neostigmine had a more potent antinociceptive effect in female rats challenged with thermal stimuli, which could be partially reversed by mecamylamine in females, but not males, whereas capsaicin induced pain did not show any sex-differences in neostigmine analgesia (Chiari et al., 1999; Lavand'homme and Eisenach, 1999). In the current study, no difference in cell-type specific responses were observed between genders and mecamylamine was effective at reducing nAChR-mediated acetylcholine responses in male rat dorsal horn neurons, which suggests that the sex differences are not due to different properties of these neuronal subtypes.

Radial neurons have been reported in a number of studies, with varyied descriptions of dendritic length, which may suggest this group includes a number of subpopulations. To further define the effect of ACh on radial neurons, we recorded from the Tac1 positive radial neuron subtype in mouse spinal cord. Radial neurons are thought to be excitatory, as they express the vesicular glutamate transporter VGLUT2 but not the GABA-synthesizing enzyme GAD (Punnakkal et al., 2014; Heinke et al., 2004). Grudt and Perl (2002) described radial neurons has having with soma sizes of 17.50 ± 0.50–19.40 ± 0.87 μm, with dendritic arbor dimensions of 87.1 ± 3.83 μm in the dorsoventral (DV) axis and 178 ± 20.1 μm in the rostrocaudal (RC) direction. However, they reported that in some of the radial neurons they visualized in parasagittal sections, the dendritic arbor appeared to be nearly circular. Action potential firing in these radial neurons were delayed from the onset of the depolarizing step and then irregular or short in duration (Grudt and Perl, 2002). Yasaka et al. (2010) reported that radial neurons are glutamatergic, also with delayed firing, but measured a larger range in dendrite lengths with 59–157 μm (RC) and 147–271 μm (DV) (Yasaka et al., 2010). Dickie

et al. (2018) showed that Tac1 positive neurons resembled radial cells with dendrite lengths of 141.5 ± 28.9 μm (RC) by 58.0 ± 11.2 μm (DV) with somas that appear to be smaller than those reported by Grudt and Perl (2002) (Grudt and Perl, 2002; Dickie et al., 2019). Alba-Delgado et al. (2015) showed that some neurons in lamina II of the medullary dorsal horn that express PKC-γ have radial morphology and dendritic arbors of 79.6 + 6 μm (DV) and 149.2 + 13 (RV), however these neurons do not exhibit delayed firing, with many showing single spike firing activity, which in some cases changed to phasic activity with higher currents (Alba-Delgado et al., 2015). Although we did not measure dendritic arbor length in this study, we are able to compare firing patterns, which in the rat radial neuron group were a mix of single spike neurons and delayed neurons. This may suggest that we recorded from both the single-spike PKC-γ expressing neurons Alba-Delgado et al. (2015) and other radial types described by Grudt and Perl (2002), Yasaka et al. (2010) and Dickie et al. (2018) that exhibit delayed firing (Grudt and Perl, 2002; Yasaka et al., 2010; Dickie et al., 2019; Alba--Delgado et al., 2015). The responses we observed to ACh were not significantly different in the rat radial neuron group to the mouse Tac1 positive neuron group.

In experiments using marmoset spinal cord, we found that primate lamina II neurons respond in much the same way as rat neurons and had similar firing properties, rheobase and resting membrane potentials. Early studies investigating ChAT immunostaining in monkey spinal cord failed to show the presence of ChAT positive neurons in the primate dorsal horn, which suggested that this region was devoid of cholinergic neurons (Pawlowski et al., 2013). However, the presence of a plexus of cholinergic fibers was later shown by Pawlowski et al. (2013) in macaque spinal cord (Pawlowski et al., 2013). Interestingly, this study also showed that the morphological features of the cholinergic neurons from lamina II of the macaque spinal cord are islet neurons, which suggests this group of neurons both respond to and release ACh. Although the cholinergic neurons are located in a different region of the dorsal horn in macaque and rodent, the similarities between primate and rodent spinal cord activity and responses in this study show these nociceptive circuits studied in great detail in rodent are relevant to primate as far in the aspects investigated to-date. However, it is not yet known whether the cholinergic neurons in marmoset are located in lamina II or in deeper lamina as in the rodent spinal cord. Nevertheless, the findings of this study may contribute to our understanding of how individual neurons within dorsal horn circuits respond to ACh.

Funding

This research was funded by the Australian National Health and Medical Research Council (NHMRC), grant numbers APP1139591, APP1139586 and APP1125877 and the Australian Research Council (ARC) grant number DP190102854.

CRediT author contribution statement

Matthew J. Sykes: Formal analysis, Investigation, Writing – original draft, All authors have read and agreed to the published version of the manuscript. **Orsolya S. Kekesi:** Investigation, All authors have read and agreed to the published version of the manuscript. **Yan T. Wong:** Resources, All authors have read and agreed to the published version of the manuscript. **Fei-Yue Zhao:** Supervision, All authors have read and agreed to the published version of the manuscript. **David Spanswick:** Conceptualization, Supervision, Writing – review & editing, All authors have read and agreed to the published version of the manuscript. **Wendy L. Imlach:** Conceptualization, Methodology, Formal analysis, Investigation, Writing – original draft, Writing – review & editing, Visualization, Supervision, Project administration, Funding acquisition, All authors have read and agreed to the published version of the manuscript.

Declaration of competing interest

The authors declare no conflict of interest.

References

Aceto, M.D., et al., 1986. The spinal cord as a major site for the antinociceptive action of nicotine in the rat. Neuropharmacology 25 (9), 1031–1036.
Alba-Delgado, C., et al., 2015. Subpopulations of PKCgamma interneurons within the medullary dorsal horn revealed by electrophysiologic and morphologic approach. Pain 156 (9), 1714–1728.
Baba, H., et al., 1998. Muscarinic facilitation of GABA release in substantia gelatinosa of the rat spinal dorsal horn. J. Physiol. 508 (Pt 1), 83–93.
Balachandar, A., Prescott, S.A., 2018. Origin of heterogeneous spiking patterns from continuously distributed ion channel densities: a computational study in spinal dorsal horn neurons. J. Physiol. 596 (9), 1681–1697.
Bellier, J.P., Kimura, H., 2007. Acetylcholine synthesis by choline acetyltransferase of a peripheral type as demonstrated in adult rat dorsal root ganglion. J. Neurochem. 101 (6), 1607–1618.
Chen, S.R., et al., 2010. Dynamic control of glutamatergic synaptic input in the spinal cord by muscarinic receptor subtypes defined using knockout mice. J. Biol. Chem. 285 (52), 40427–40437.
Chiari, A., et al., 1999. Sex differences in cholinergic analgesia I: a supplemental nicotinic mechanism in normal females. Anesthesiology 91 (5), 1447–1454.
Coggeshall, R.E., Carlton, S.M., 1997. Receptor localization in the mammalian dorsal horn and primary afferent neurons. Brain Res Brain Res Rev 24 (1), 28–66.
Cordero-Erausquin, M., et al., 2004. Nicotine differentially activates inhibitory and excitatory neurons in the dorsal spinal cord. Pain 109 (3), 308–318.
Cucchiaro, G., et al., 2008. Analgesic effects of Sazetidine-A, a new nicotinic cholinergic drug. Anesthesiology 109 (3), 512–519.
Demuro, A., et al., 2001. Inhibition of nicotinic acetylcholine receptors by bicuculline. Neuropharmacology 41 (7), 854–861.
Dhanasobhon, D., et al., 2021. Enhanced analgesic cholinergic tone in the spinal cord in a mouse model of neuropathic pain. Neurobiol. Dis. 155, 105363.
Dickie, A.C., et al., 2019. Morphological and functional properties distinguish the substance P and gastrin-releasing peptide subsets of excitatory interneuron in the spinal cord dorsal horn. Pain 160 (2), 442–462.
Fiorino, D.F., Garcia-Guzman, M., 2012. Muscarinic pain pharmacology: realizing the promise of novel analgesics by overcoming old challenges. Handb. Exp. Pharmacol. (208), 191–221.
Garcia-Colunga, J., Miledi, R., 1999. Modulation of nicotinic acetylcholine receptors by strychnine. Proc. Natl. Acad. Sci. U. S. A. 96 (7), 4113–4118.
Genzen, J.R., McGehee, D.S., 2003. Short- and long-term enhancement of excitatory transmission in the spinal cord dorsal horn by nicotinic acetylcholine receptors. Proc. Natl. Acad. Sci. U. S. A. 100 (11), 6807–6812.
Genzen, J.R., McGehee, D.S., 2005. Nicotinic modulation of GABAergic synaptic transmission in the spinal cord dorsal horn. Brain Res. 1031 (2), 229–237.
Graham, B.A., Brichta, A.M., Callister, R.J., 2007. Moving from an averaged to specific view of spinal cord pain processing circuits. J. Neurophysiol. 98 (3), 1057–1063.
Grudt, T.J., Perl, E.R., 2002. Correlations between neuronal morphology and electrophysiological features in the rodent superficial dorsal horn. J. Physiol. 540 (Pt 1), 189–207.
Gutierrez-Mecinas, M., et al., 2017. Preprotachykinin A is expressed by a distinct population of excitatory neurons in the mouse superficial spinal dorsal horn including cells that respond to noxious and pruritic stimuli. Pain 158 (3), 440–456.
Haring, M., et al., 2018. Neuronal atlas of the dorsal horn defines its architecture and links sensory input to transcriptional cell types. Nat. Neurosci. 21 (6), 869–880.
Harris, J.A., et al., 2014. Anatomical characterization of Cre driver mice for neural circuit mapping and manipulation. Front. Neural Circ. 8, 76.
Heinke, B., et al., 2004. Physiological, neurochemical and morphological properties of a subgroup of GABAergic spinal lamina II neurones identified by expression of green fluorescent protein in mice. J. Physiol. 560 (Pt 1), 249–266.
Hoglund, A.U., Baghdoyan, H.A., 1997. M2, M3 and M4, but not M1, muscarinic receptor subtypes are present in rat spinal cord. J. Pharmacol. Exp. Therapeut. 281 (1), 470–477.
Imlach, W.L., et al., 2016. Glycinergic dysfunction in a subpopulation of dorsal horn interneurons in a rat model of neuropathic pain. Sci. Rep. 6, 37104.
Iwamoto, E.T., Marion, L., 1993. Adrenergic, serotonergic and cholinergic components of nicotinic antinociception in rats. J. Pharmacol. Exp. Therapeut. 265 (2), 777–789.
Khan, I.M., et al., 1998. Nociceptive and antinociceptive responses to intrathecally administered nicotinic agonists. Neuropharmacology 37 (12), 1515–1525.
Kichko, T.I., et al., 2013. Bimodal concentration-response of nicotine involves the nicotinic acetylcholine receptor, transient receptor potential vanilloid type 1, and transient receptor potential ankyrin 1 channels in mouse trachea and sensory neurons. J. Pharmacol. Exp. Therapeut. 347 (2), 529–539.
Kiyosawa, A., et al., 2001. Nicotine facilitates glycine release in the rat spinal dorsal horn. J. Physiol. 536 (Pt 1), 101–110.
Laing, I., et al., 1994. Subpopulations of GABAergic neurons in laminae I-III of rat spinal dorsal horn defined by coexistence with classical transmitters, peptides, nitric oxide synthase or parvalbumin. Neuroscience 61 (1), 123–132.
Lauretti, G.R., et al., 1998. A multi-center study of intrathecal neostigmine for analgesia following vaginal hysterectomy. Anesthesiology 89 (4), 913–918.
Lavand'homme, P.M., Eisenach, J.C., 1999. Sex differences in cholinergic analgesia II: differing mechanisms in two models of allodynia. Anesthesiology 91 (5), 1455–1461.

Li, D.P., et al., 2002. Role of presynaptic muscarinic and GABA(B) receptors in spinal glutamate release and cholinergic analgesia in rats. J. Physiol. 543 (Pt 3), 807–818.
Madisen, L., et al., 2010. A robust and high-throughput Cre reporting and characterization system for the whole mouse brain. Nat. Neurosci. 13 (1), 133–140.
Matsubayashi, H., et al., 1998. Strychnine: a potent competitive antagonist of alpha-bungarotoxin-sensitive nicotinic acetylcholine receptors in rat hippocampal neurons. J. Pharmacol. Exp. Therapeut. 284 (3), 904–913.
Mesnage, B., et al., 2011. Morphological and functional characterization of cholinergic interneurons in the dorsal horn of the mouse spinal cord. J. Comp. Neurol. 519 (16), 3139–3158.
Naser, P.V., Kuner, R., 2017. Molecular, cellular and circuit basis of cholinergic modulation of pain. Neuroscience 387, 135–148.
Nicolodi, M., et al., 2002. Central cholinergic challenging of migraine by testing second-generation anticholinesterase drugs. Headache 42 (7), 596–602.
Pawlowski, S.A., et al., 2013. A novel population of cholinergic neurons in the macaque spinal dorsal horn of potential clinical relevance for pain therapy. J. Neurosci. 33 (9), 3727–3737.
Peirs, C., Dallel, R., Todd, A.J., 2020. Recent advances in our understanding of the organization of dorsal horn neuron populations and their contribution to cutaneous mechanical allodynia. J. Neural. Transm. 127 (4), 505–525.
Picciotto, M.R., Higley, M.J., Mineur, Y.S., 2012. Acetylcholine as a neuromodulator: cholinergic signaling shapes nervous system function and behavior. Neuron 76 (1), 116–129.
Punnakkal, P., et al., 2014. Morphological, biophysical and synaptic properties of glutamatergic neurons of the mouse spinal dorsal horn. J. Physiol. 592 (4), 759–776.
Rashid, M.H., Ueda, H., 2002. Neuropathy-specific analgesic action of intrathecal nicotinic agonists and its spinal GABA-mediated mechanism. Brain Res. 953 (1–2), 53–62.
Rashid, M.H., et al., 2006. Tonic inhibitory role of alpha4beta2 subtype of nicotinic acetylcholine receptors on nociceptive transmission in the spinal cord in mice. Pain 125 (1–2), 125–135.
Ribeiro-da-Silva, A., De Koninck, Y., 2008. Morphological and Neurochemical Organization of the Spinal Dorsal Horn, vol. 5, pp. 279–310.
Stewart, W., Maxwell, D.J., 2003. Distribution of and organisation of dorsal horn neuronal cell bodies that possess the muscarinic m2 acetylcholine receptor. Neuroscience 119 (1), 121–135.
Stornetta, R.L., et al., 2013. Cholinergic neurons in the mouse rostral ventrolateral medulla target sensory afferent areas. Brain Struct. Funct. 218 (2), 455–475.
Takeda, D., et al., 2003. Modulation of inhibitory synaptic activity by a non-alpha4beta2, non-alpha7 subtype of nicotinic receptors in the substantia gelatinosa of adult rat spinal cord. Pain 101 (1–2), 13–23.
Todd, A.J., 2010. Neuronal circuitry for pain processing in the dorsal horn. Nat. Rev. Neurosci. 11 (12), 823–836.
Todd, A.J., 2017. Identifying functional populations among the interneurons in laminae I-III of the spinal dorsal horn. Mol. Pain 13, 1744806917693003.
Wang, X.L., et al., 2006. Dynamic regulation of glycinergic input to spinal dorsal horn neurones by muscarinic receptor subtypes in rats. J. Physiol. 571 (Pt 2), 403–413.
Yalcin, I., et al., 2011. Nociceptive thresholds are controlled through spinal beta2-subunit-containing nicotinic acetylcholine receptors. Pain 152 (9), 2131–2137.
Yasaka, T., et al., 2010. Populations of inhibitory and excitatory interneurons in lamina II of the adult rat spinal dorsal horn revealed by a combined electrophysiological and anatomical approach. Pain 151 (2), 475–488.
Yoon, S.Y., et al., 2005. Intrathecal neostigmine reduces the zymosan-induced inflammatory response in a mouse air pouch model via adrenomedullary activity: involvement of spinal muscarinic type 2 receptors. Neuropharmacology 49 (3), 275–282.
Young, T., et al., 2008. Spinal alpha3beta2* nicotinic acetylcholine receptors tonically inhibit the transmission of nociceptive mechanical stimuli. Brain Res. 1229, 118–124.
Zhang, H.M., et al., 2005. M2, M3, and M4 receptor subtypes contribute to muscarinic potentiation of GABAergic inputs to spinal dorsal horn neurons. J. Pharmacol. Exp. Therapeut. 313 (2), 697–704.
Zhang, H.M., Chen, S.R., Pan, H.L., 2007. Regulation of glutamate release from primary afferents and interneurons in the spinal cord by muscarinic receptor subtypes. J. Neurophysiol. 97 (1), 102–109.
Zhu, M.H., et al., 2011. Muscarinic activation of Ca2+-activated Cl- current in interstitial cells of Cajal. J. Physiol. 589 (Pt 18), 4565–4582.
Zhuo, M., Gebhart, G.F., 1991. Tonic cholinergic inhibition of spinal mechanical transmission. Pain 46 (2), 211–222.